


Cite this: *J. Mater. Chem. A*, 2020, **8**, 12285Received 18th April 2020
Accepted 4th June 2020

DOI: 10.1039/d0ta04146g

rsc.li/materials-a

Ternary ZIF-8-derived dual-metal CoCu nanoparticles in porous carbon polyhedra as efficient catalysts for methanol oxidation†

Chaoyun Tang ^{abc} and Tewodros Asefa ^{*bc}

Novel ternary-metallic ZIFs are synthesized in one-step. They are then converted into highly catalytically active, three-dimensional nanoporous, polyhedral-shaped carbon microparticles containing CoCu dual-metal nanoparticles that can efficiently electrocatalyze the methanol oxidation reaction (MOR). The Co-rich material shows among the highest mass activities reported for non-noble metal MOR electrocatalysts.

Direct methanol fuel cells (DMFCs) have attracted tremendous interest due to their high energy conversion efficiency, low operating temperature, and great potential to serve as energy sources for portable electronic devices and electric vehicles.^{1,2}

DMFCs are also a promising energy conversion technology because of the high energy content of liquid methanol (6100 W h kg⁻¹), methanol's ability to serve as a fuel storage medium under ambient conditions, and the ease of deployment of such fuel cells. The performance of DMFCs depends strongly on the efficiency of the methanol oxidation reaction (MOR) occurring in them. Although noble-metals, such as Pd or Pt, are well-recognized as efficient electrocatalysts for the MOR,³ their practical application in DMFCs is constrained by the high cost and limited supply of these metals.⁴ Thus, alternative, inexpensive noble metal-free electrocatalysts with high activity for the MOR need to be developed to scale-up DMFCs.^{5,6}

Owing to their high specific surface areas,⁷ metal-organic frameworks (MOFs) are ideal for application in catalysis, drug delivery, and energy storage and conversions.^{8–10} However, most MOFs cannot be directly adopted as electrocatalysts because of

their low electrical conductivity and poor chemical stability.¹¹ Recently, it has been shown that MOFs could be converted into various conductive carbon-based materials *via* pyrolysis.^{12–14} The resulting materials can also inherit some of the MOFs' structural merits, such as the high surface area, well-defined morphology, and high surface-to-volume ratio.¹⁵ Moreover, they are more chemically stable than MOFs, and some show electrocatalytic activity for different reactions depending on the types and amounts of metals in them. Some have also been demonstrated to have applications as supercapacitors.^{16,17}

Zeolitic imidazolate frameworks (ZIFs) are a class of MOFs that are built from four-coordinated transition metal ions (Zn²⁺, Co²⁺, Fe²⁺ or Cu²⁺) and imidazolate linkers.^{18,19} Zn-based ZIFs (ZIF-8) and Co-based ZIFs (ZIF-67) were the two most widely studied ZIFs in the past few decades.^{20,21} Both can easily be synthesized at room temperature,²² and their morphology and structures can be tailored using various mild solvothermal conditions.^{23,24} Both ZIFs are structurally similar to aluminosilicate zeolites. While the Zn²⁺ or Co²⁺ ions in ZIFs are like the Si atoms in aluminosilicate zeolites, the imidazoles in ZIFs are akin to the O atoms in zeolites. Recently, a Zn/Co mixed ZIF was synthesized and used as a precursor to produce single-atom catalysts (SACs).²⁵ In this ZIF, Co²⁺ ions were spatially separated by 2-methylimidazolate linkers and Zn²⁺ ions. When the ZIF was pyrolyzed, Zn evaporated and a carbon material with single Co atoms was obtained.²⁶ We thought that ternary-metallic ZIF materials would give bi-metallic analogues that could serve as more effective catalysts due to the synergistic effects between the two metals. Specifically, we expected that a ternary ZIF composed of Zn/Co/M could be transformed into carbon materials containing Co/M dual-metal nanoparticles.

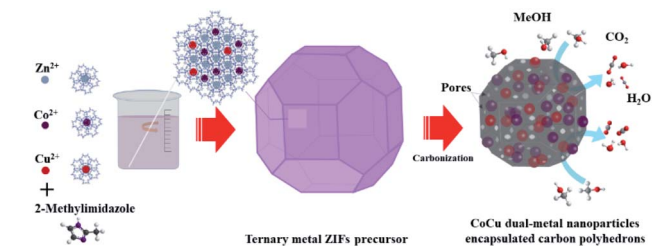
To this end, we report here 3D nanoporous polyhedral-shaped carbon microparticles possessing CoCu nanoparticles derived from ternary ZIFs that are rationally prepared in one-step from different ratios of Zn²⁺, Co²⁺, Cu²⁺ and imidazolate ions (Scheme 1). The synthetic details can be found in the ESI.† The products, which are named carbonized ZIFs (or CZIFs), have high surface areas, nanopores, and good conductivity. The

^aHoffmann Institute of Advanced Materials, Shenzhen Polytechnic, 7098 Liuxian Boulevard, Shenzhen 518060, China

^bDepartment of Chemistry and Chemical Biology, Rutgers, The State University of New Jersey, 610 Taylor Road, Piscataway, New Jersey 08854, USA. E-mail: tasefa@chem.rutgers.edu

^cDepartment of Chemical & Biochemical Engineering, Rutgers, The State University of New Jersey, 98 Brett Road, Piscataway, New Jersey 08854, USA

† Electronic supplementary information (ESI) available. See DOI: 10.1039/d0ta04146g



Scheme 1 Schematic illustration of the synthetic procedure used to produce ternary ZIFs containing Zn, Co and Cu in different ratios, and then 3D nanoporous carbon polyhedron microparticles containing dual-metal (CoCu) nanoparticles (CZIFs).

CZIF materials possessing a relatively higher amount of Co than Cu also show excellent electrocatalytic activity for the MOR, with activity among the best mass activities reported for noble metal-free MOR catalysts to date.

First, a series of ternary metal ZIFs with different mole ratios of Zn, Co and Cu is synthesized *via* a procedure commonly used to synthesize ZIF-8,^{27,28} with a slight modification. The ZIFs are then pyrolyzed at 900 °C in a N₂ atmosphere to produce CZIFs. During pyrolysis, the Zn atoms evaporate above 800 °C and leave nanopores in their places. The loss of Zn from Zn-based MOFs was reported to create porous structures and free N sites that can stabilize single metal atoms.²³ In our case, similar structures, albeit with Co/Cu bimetallic nanoparticles, are formed. No metallic Zn is observed in the materials under these conditions; if any Zn is observed, ZnO is formed at a lower pyrolysis temperature (*e.g.*, 600 °C). The relative amounts of Co and Cu nanoparticles formed in the CZIFs are indirectly adjusted by varying the ratio of Co²⁺ and Cu²⁺ ions used to make the parent ZIFs. After characterization of the materials, the electrocatalytic properties of CZIFs for the MOR are studied.

All ZIF materials show similar X-ray diffraction (XRD) patterns that correspond to the typical sodalite crystal structures of ZIFs (Fig. S1†). Their field-emission scanning electron microscope (FESEM) images (Fig. S2,† left panels) show microparticles with a polyhedral shape and smooth surfaces, which is the characteristic morphology of ZIF materials. Meanwhile, the XRD patterns of CZIF materials (Fig. 1) show a peak at 26° which corresponds to the (002) plane of graphitic carbon. The peaks at 44.2°, 51.5° and 75.8° are indexed to the (111), (200) and (220) planes of metallic Co (JCPDS Card No. 89-7093) and those at 43.4°, 50.5° and 74.3° are indexed to the (111), (200) and (220) planes of metallic Cu (JCPDS Card No. 65-9743). The intensities of the peaks associated with Co increase as the relative amount of Co²⁺ in the parent ZIFs is increased; conversely, the intensities of the Cu peaks decrease as the relative amount of Cu in the parent ZIFs is decreased. No peaks associated with metallic Zn are seen in the XRD patterns of CZIFs because Zn has evaporated during pyrolysis.

The materials are then characterized by electron microscopy (Fig. 2 and S2–S4†). FESEM images of CZIF materials (Fig. 2a, e and S2†, right panels) also show polyhedral microparticles, except that they are slightly shrunk due to the high temperature treatment.^{29,30} To further investigate their morphology and

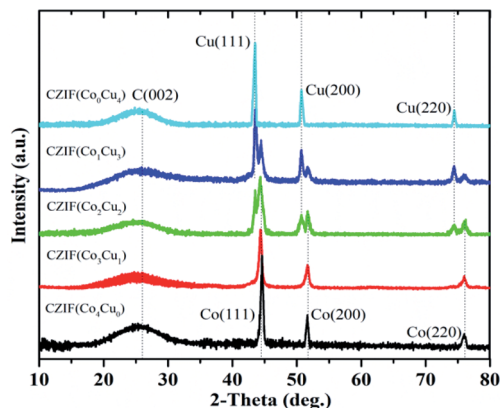


Fig. 1 Powder XRD patterns of CZIF materials containing different relative amounts of Co and Cu. The materials are obtained by pyrolyzing ZIF materials possessing different mole ratios of Zn, Co and Cu at 900 °C.

structure, their high resolution transmission electron microscope (HRTEM) images are acquired (Fig. 2b, c, f, g and S3†). HRTEM images show nanoporous polyhedral-shaped carbon microparticles containing nanoparticles of 5–10 nm in size. HRTEM images of CZIF(Co₄Cu₀) and CZIF(Co₀Cu₄) (Fig. S3†) show lattice fringes with interplanar spacings of 0.205 nm and 0.208 nm, which correspond to the (111) planes of Co and Cu, respectively. The selected area electron diffraction (SAED) pattern of CZIF(Co₄Cu₀) displays diffraction rings corresponding to the (111), (200) and (220) planes of Co while that of CZIF(Co₀Cu₄) shows diffraction rings corresponding to the (111), (200) and (220) planes of Cu (Fig. S4†). As Co and Cu possess similar lattice fringes, distinguishing them in the SAED patterns of the CZIF materials containing both Co and Cu is difficult.

Meanwhile, elemental mapping images of CZIF(Co₃Cu₁) and CZIF(Co₁Cu₃), obtained with a high-resolution energy-dispersive X-ray spectrometer (EDS) (Fig. 2d and h, respectively), show homogeneously distributed Co, Cu and C atoms over the entire material. In addition, the more dominant metal is seen distinctively localized in certain regions with the less prominent one residing around it. Such types of bimetallic nanoparticles within nanoporous conductive carbon matrices can be expected to provide good binding sites for different reactants and intermediates and promote various electrochemical reactions.

The BET surface areas of the series of ternary-metallic ZIF materials and the corresponding CZIF materials are measured using N₂ adsorption–desorption isotherms (Fig. S5†), and the values are listed in Table S1.† The ternary ZIFs show high surface areas, just like many other previously reported ZIF materials^{7,18,19} and other hybrid porous materials.³¹ Compared with the surface areas of ZIFs, those of CZIF materials are lower (298 m² g^{−1} for CZIF(Co₃Cu₁), 275 m² g^{−1} for CZIF(Co₁Cu₃), *etc.*); this is to be expected because of the shrinkage of the pores due to the thermal treatment. Nevertheless, the CZIF materials still possess relatively high surface areas, with values higher than those of other notable MOF-derived electrocatalysts (116.2

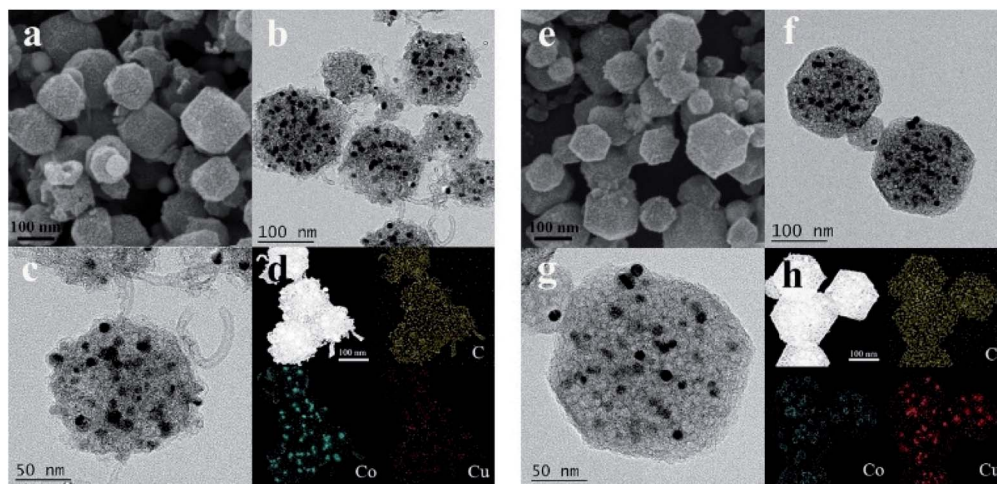


Fig. 2 (a) FESEM, (b and c) TEM and (d) EDS elemental mapping images of CZIF(Co₃Cu₁). (e) FESEM, (f and g) TEM and (h) EDS elemental mapping images of CZIF(Co₁Cu₃).

m² g⁻¹),¹¹ supercapacitors (196 m² g⁻¹),³² etc.^{11,33} The pores in CZIF materials, determined by the BJH method (Fig. S6†), are micropores and mesopores, with average sizes of 1 nm and 7–8 nm, respectively. Due to their large surface area and nanopores, the metallic nanoparticles inside CZIFs should be accessible to electrolytes and reactants during electrocatalysis.

The composition, electronic states and nature of bonding of the elements in CZIF materials are investigated by X-ray photoelectron spectroscopy (XPS). The survey XPS spectrum of a typical CZIF material, CZIF (Co₃Cu₁), (Fig. S7†) shows the existence of Co, Cu, O, N and C elements in the material. The presence of the O atoms is most likely due to the surface oxidation of the sample in air. In the XPS spectra of Co 2p and Cu 2p peaks of CZIF materials (Fig. 3), only a peak associated with Co⁰ at 778.2 eV, with a satellite peak at 786.1 eV, and a peak associated with Cu⁰ at 932.7 eV are observed. This means metallic Co and Cu are present in CZIFs. The intensities of these peaks vary according to the mole ratio of Co/Cu used to make their parent ZIFs. This is in good agreement with the electron microscopy and XRD results discussed earlier. Quantitative analysis of the elements in each material is carried out by EDS spectroscopy (Fig. S8 and Table S2†). The results show that the relative amount of Co in the CZIFs is more than what is used to

make the corresponding ZIFs, implying that Co conforms with, or makes it into, a ZIF structure better than Cu.

Next, the electrocatalytic activity of CZIF materials for the MOR is measured by cyclic voltammetry at a scan rate of 50 mV s⁻¹ in N₂-purged 1.0 M KOH solutions with and without 1.0 M MeOH (Fig. 4a and b). In order to eliminate the effect of double-layer capacitance, the data are normalized to mass activity.⁵ During the experiment, CZIF(Co₄Cu₀), which has no Cu, gives an anodic current related to the oxygen evolution reaction (OER), rather than to the MOR. This is not surprising given cobalt's known electrocatalytic activity toward the OER.^{34,35} The

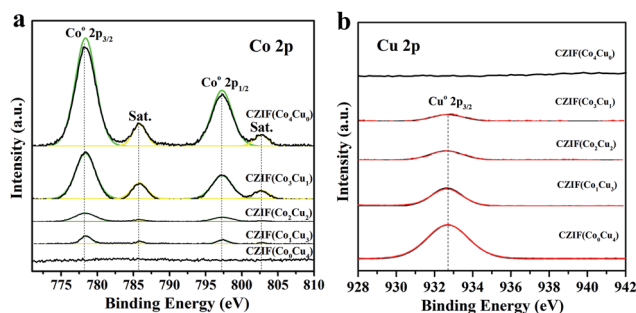


Fig. 3 XPS spectra of a series of CZIF materials possessing different mole ratios of Co and Cu, as indicated with the numbers in brackets.

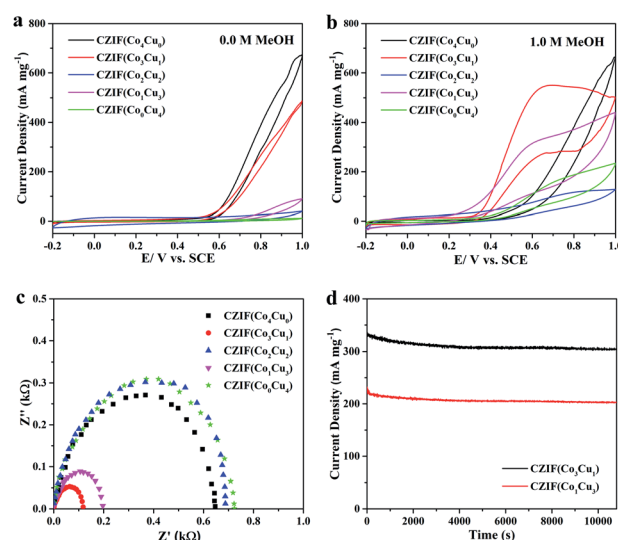


Fig. 4 (a) Mass-normalized CV curves obtained for different CZIF catalysts in 1 M KOH solution (without MeOH). (b) CV curves for electro-oxidation of the MOR over the different catalysts in 1 M KOH solution containing 1 M MeOH. The tests are all performed at a scan rate of 50 mV s⁻¹. (c) Nyquist plots of EIS for the series of CZIF catalysts at 1 V vs. SCE. (d) Chronoamperograms of the MOR over CZIF(Co₃Cu₁) and CZIF(Co₁Cu₃) electrodes at 0.5 V vs. SCE in 1 M KOH containing 1.0 M MeOH for 3 h.

anodic current density barely increases after the addition of MeOH, indicating that Co has weak activity for the MOR.³⁶ On the other hand, CZIF(Co₀Cu₄), which has no Co, barely gives an anodic current associated with the OER.^{37,38} However, upon addition of some MeOH, it gives an anodic current.³⁹ This indicates that the CZIF containing only Cu shows little electrocatalytic activity for the OER, compared to the MOR. Interestingly, in the case of CZIF(Co₃Cu₁) and CZIF(Co₁Cu₃), not only do they give anodic current density with the addition of MeOH but also their current density increases sharply as more MeOH is added. In particular, CZIF(Co₃Cu₁) gives the highest mass activity, namely, 551 A g⁻¹ at a small potential of 0.695 V vs. SCE. The corresponding value for CZIF(Co₁Cu₃) is 314 A g⁻¹. As these mass activities may be partly contributed by the OER, the baseline current obtained in the absence of MeOH (or due to the OER) is subtracted and the mass activity only due to the MOR is determined. The value for CZIF(Co₃Cu₁) is found to be 419 A g⁻¹. This is not only very high but also among the best mass activities reported for noble metal-free MOR electrocatalysts to date (see Table S3†). The mass activity of CZIF(Co₁Cu₃) is also high, with a value of 310.6 A g⁻¹, albeit substantially lower than that of CZIF(Co₃Cu₁). More interestingly, CZIF(Co₂Cu₂), which is synthesized from a 1 : 1 mole ratio of Co and Cu, barely shows any catalytic activity for the MOR (nor for the OER).

These results reveal that not only the presence of both Co and Cu but also their mole ratios are very important in the catalytic activities of CZIF materials reported herein. The results also indicate that synergistic electrochemical processes between Co and Cu must have helped CZIF(Co₃Cu₁) and CZIF(Co₁Cu₃) to catalyze the MOR. This is not surprising since it is difficult for a single type of metal to oxidize MeOH well⁴⁰ because it cannot exert a weak binding affinity to both carbonaceous species (CO*) (meaning activation of MeOH) and to hydroxyl species (OH*) (meaning activation of H₂O). Thus, catalysts possessing two different metals that can perform these two processes are sought after to effectively catalyze the MOR, just like the PtRu alloy, a well-known MOR catalyst.^{41,42} Both Co and Cu are considered among the best non-noble metal catalysts to carry out the two above-mentioned processes needed for the MOR.^{43,44} This is not surprising given cobalt's similar adsorption free energy for CO* to platinum's, and cobalt's strong binding affinity to CO*, which means Co can favor the formation of CO* from MeOH. However, Co has a strong binding affinity also to OH* and can thus activate water to form OH* species. The OH* species can then be oxidized to oxygen (O*) species, proceeding to O₂. However, the O* species binds Co so strongly that it can neither easily oxidize CO* nor can it poison cobalt's surface. On the other hand, Cu has a moderate binding affinity to CO*. Thus, it can activate MeOH without getting poisoned by CO*. Moreover, as Cu has a moderate binding affinity to OH*, it is also unable to catalyze the OER. These results collectively mean that having optimal amounts of Co and Cu in CZIFs co-drives well the two processes critical to the MOR.

The electrocatalytic activities of the materials for the MOR at different concentrations of MeOH are also evaluated. The CV curves of CZIF(Co₃Cu₁) and CZIF(Co₁Cu₃) for the MOR in 1 M

KOH solutions containing 0.0, 0.5, 1.0, 1.5 and 2.0 M MeOH are displayed in Fig. S9.† The results show the typical electrochemical responses associated with the MOR. The oxidation peak current density is proportional to the concentration of MeOH, indicating that a diffusion-controlled process is at work.⁴ The oxidation peaks show a slight positive shift as the concentration of MeOH is increased. This is because a slightly higher oxidation potential is needed as more MeOH is adsorbed on the catalyst's surface.

To gain insight into the kinetics of the electrochemical processes of the MOR on the catalysts, the charge transfer resistance (R_{ct}) of the series of CZIF catalysts is measured. Fig. 4c shows the EIS Nyquist plots of the catalysts at a potential of 1 V vs. SCE. The values of R_{ct} of CZIF(Co₃Cu₁) and CZIF(Co₁Cu₃) are much smaller than those of the other CZIF catalysts. This suggests that a more efficient electron transport process and favorable MOR kinetics are possible at the interfaces between these two CZIF electrocatalysts and the electrolyte.

To further probe other possible features endowing the CZIF materials with excellent electrocatalytic performances for the MOR, their electrochemical double-layer capacitance (C_{dl}), which is directly correlated with the electrochemically active area (ECSA), is measured (see Fig. S10 and Table S4†). Generally, a material should have a good C_{dl} or ECSA to be a good electrocatalyst. All CZIF materials show high C_{dl} values, unsurprisingly due to their high specific surface areas. Moreover, the two monometallic CZIF materials, *i.e.*, CZIF(Co₄Cu₀) and CZIF(Co₀Cu₄), have relatively higher C_{dl} (with values of 30.77 mF cm⁻² and 28.28 mF cm⁻², respectively) whereas the two CZIF materials containing dual-metallic nanoparticles, *i.e.*, CZIF(Co₃Cu₁) and CZIF(Co₁Cu₃), have slightly lower C_{dl} (with values of 27.83 mF cm⁻² and 25.67 mF cm⁻², respectively).

These results suggest that CZIF(Co₃Cu₁), the material containing a relatively higher amount of Co, has high conductivity, low charge transfer resistance (R_{ct}) and a relatively higher surface area, plus shows the more efficient electron transport process from Co to Cu (just like Ni to Cu in previously reported materials).¹ This may be why it exhibits the best catalytic activity for the MOR among the CZIF materials. The structures of the CZIF materials vary because Co and Cu exert different catalytic effects during carbonization.^{45–47} For example, Co tends to give less graphitic/crystalline carbon, and conversely a more porous structure, than Cu.

Finally, chronoamperometry was used to determine the stability of CZIF(Co₃Cu₁) and CZIF(Co₁Cu₃) materials during electrocatalytic MOR in 1 M KOH solution containing 1 M MeOH at a potential of 0.5 V vs. SCE for 3 h (Fig. 4d). In the chronoamperogram, a slight drop in current density is observed in both cases. The reduction in current density in the beginning must be because of the fast reaction kinetics, where the active sites are free of adsorbed MeOH molecules. The adsorption of additional MeOH molecules is governed by how quickly the electrocatalytic sites on the catalyst's surfaces become free as MeOH oxidation takes place. However, the subsequent slight drop in current density could be primarily due to the slight poisoning of the catalysts. Nevertheless, CZIF (Co₃Cu₁) retains

90.4% current density and CZIF(Co₁Cu₃) maintains 87.7% current density after 3 h of the MOR. So, both CZIFs have reasonably good durability for the MOR, which must be due to the weak binding of CO to Cu, which is also why Cu is commonly used as a water-gas shift catalyst.⁴⁸

Conclusions

In summary, 3D carbon polyhedra containing dual-metal CoCu nanoparticles are synthesized by first preparing in one-step ternary-metallic ZIFs containing different relative amounts of Zn, Co and Cu and then pyrolyzing them at 900 °C in a N₂ atmosphere. Detailed electrochemical measurements showed that the as-synthesized carbonized ZIFs (or CZIF materials) containing a slightly higher amount of the two metal nanoparticles, especially Co, exhibited excellent and stable electrocatalytic activities for the MOR. However, the materials containing only one of the two metal nanoparticles as well as roughly similar amounts of them showed weak or no catalytic activities for the MOR. In particular, CZIF materials containing a relatively higher amount of Co exhibited among the highest electrocatalytic activities reported for non-noble metal MOR catalysts, with high mass activity. This work can be extended to synthesize other desirable advanced functional electrocatalysts from well-designed and prepared MOFs with unique structures and tailored compositions. Such noble metal-free MOR catalysts are appealing for use in large-scale DMFCs in portable devices and auxiliary power units.

Conflicts of interest

There are no conflicts to declare.

Acknowledgements

CT acknowledges the financial support from the National Natural Science Foundation of China (51702220) and the support through the Post-doctoral Later-stage Foundation Project of Shenzhen Polytechnic (6019211006K).

References

- X. Cui, P. Xiao, J. Wang, M. Zhou, W. Guo, Y. Yang, Y. He, Z. Wang, Y. Yang, Y. Zhang and Z. Lin, *Angew. Chem., Int. Ed.*, 2017, **56**, 4488–4493.
- B. Y. Xia, H. B. Wu, X. Wang and X. W. Lou, *J. Am. Chem. Soc.*, 2012, **134**, 13934–13937.
- I. S. Pieta, A. Rath, P. Pieta, R. Nowakowski, M. Holdynski, M. Pisarek, A. Kaminska, M. B. Gawande and R. Zboril, *Appl. Catal., B*, 2019, **244**, 272–283.
- Y. Sun, Y. Zhou, C. Zhu, W. Tu, H. Wang, H. Huang, Y. Liu, M. Shao, J. Zhong, S.-T. Lee and Z. Kang, *Appl. Catal., B*, 2019, **244**, 795–801.
- Y.-P. Wu, J.-W. Tian, S. Liu, B. Li, J. Zhao, L.-F. Ma, D.-S. Li, Y.-Q. Lan and X. Bu, *Angew. Chem., Int. Ed.*, 2019, **58**, 12185–12189.
- J. Li, Z. Luo, Y. Zuo, J. Liu, T. Zhang, P. Tang, J. Arbiol, J. Llorca and A. Cabot, *Appl. Catal., B*, 2018, **234**, 10–18.
- P. Falcato, R. Ricco, C. M. Doherty, K. Liang, A. J. Hill and M. J. Styles, *Chem. Soc. Rev.*, 2014, **43**, 5513–5560.
- W. Xia, A. Mahmood, R. Zou and Q. Xu, *Energy Environ. Sci.*, 2015, **8**, 1837–1866.
- J. Hu, M. Chen, X. Fang and L. Wu, *Chem. Soc. Rev.*, 2011, **40**, 5472–5491.
- Q. Lin, X. Bu, A. Kong, C. Mao, X. Zhao, F. Bu and P. Feng, *J. Am. Chem. Soc.*, 2015, **137**, 2235–2238.
- G. Yilmaz, K. M. Yam, C. Zhang, H. J. Fan and G. W. Ho, *Adv. Mater.*, 2017, **29**, 1606814.
- Z. Li, M. Shao, L. Zhou, R. Zhang, C. Zhang, M. Wei, D. G. Evans and X. Duan, *Adv. Mater.*, 2016, **28**, 2337–2344.
- D. Zhao, J.-L. Shui, L. R. Grabstanowicz, C. Chen, S. M. Commet, T. Xu, J. Lu and D.-J. Liu, *Adv. Mater.*, 2014, **26**, 1093–1097.
- W. Zhang, Z.-Y. Wu, H.-L. Jiang and S.-H. Yu, *J. Am. Chem. Soc.*, 2014, **136**, 14385–14388.
- H. Hu, B. Guan, B. Xia and X. W. Lou, *J. Am. Chem. Soc.*, 2015, **137**, 5590–5595.
- R. R. Salunkhe, Y. V. Kaneti and Y. Yamauchi, *ACS Nano*, 2017, **11**, 5293–5308.
- H. B. Wu and X. W. Lou, *Sci. Adv.*, 2017, **3**, eaap9252.
- Q.-L. Zhu and Q. Xu, *Chem. Soc. Rev.*, 2014, **43**, 5468–5512.
- R. Wu, T. Fan, J. Chen and Y. Li, *ACS Sustainable Chem. Eng.*, 2019, **7**, 3632–3646.
- K. Shen, L. Zhang, X. Chen, L. Liu, D. Zhang, Y. Han, J. Chen, J. Long, R. Luque, Y. Li and B. Chen, *Science*, 2018, **359**, 206–210.
- B. You, N. Jiang, M. Sheng, S. Gul, J. Yano and Y. Sun, *Chem. Mater.*, 2015, **27**, 7636–7642.
- K. Zhou, B. Mousavi, Z. Luo, S. Phatanasri, S. Chaemchuen and F. Verpoort, *J. Mater. Chem. A*, 2017, **5**, 952–957.
- J. Yang, F. Zhang, H. Lu, X. Hong, H. Jiang, Y. Wu and Y. Li, *Angew. Chem., Int. Ed.*, 2015, **54**, 10889–10893.
- P. Zhang, B. Y. Guan, L. Yu and X. W. Lou, *Angew. Chem., Int. Ed.*, 2017, **56**, 7141–7145.
- P. Yin, T. Yao, Y. Wu, L. Zheng, Y. Lin, W. Liu, H. Ju, J. Zhu, X. Hong, Z. Deng, G. Zhou, S. Wei and Y. Li, *Angew. Chem., Int. Ed.*, 2016, **55**, 10800–10805.
- A. Han, B. Wang, A. Kumar, Y. Qin, J. Jin, X. Wang, C. Yang, B. Dong, Y. Jia, J. Liu and X. Sun, *Small Methods*, 2019, **3**, 1800471.
- K. Kida, M. Okita, K. Fujita, S. Tanaka and Y. Miyake, *CrystEngComm*, 2013, **15**, 1794–1801.
- X. He, C. Yang, D. Wang, S. E. Gilliland III, D.-R. Chen and W.-N. Wang, *CrystEngComm*, 2017, **19**, 2445–2450.
- Y. Liang, J. Wei, Y. X. Hu, X. F. Chen, J. Zhang, X. Y. Zhang, S. P. Jiang, S. W. Tao and H. T. Wang, *Nanoscale*, 2017, **9**, 5323–5328.
- L. He, L. Li, L. Zhang, S. Xing, T. Wang, G. Li, X. Wu, Z. Su and C. Wang, *CrystEngComm*, 2014, **16**, 6534–6537.
- Q. Chen, A. Dong, D. Wang, L. Qiu, C. Ma, Y. Yuan, Y. Zhao, N. Jia, Z. Guo and N. Wang, *Angew. Chem., Int. Ed.*, 2019, **58**, 10671–10676.

- 32 Z. Jiang, Z. Li, Z. Qin, H. Sun, X. Jiao and D. Chen, *Nanoscale*, 2013, **5**, 11770–11775.
- 33 B. Han, G. Cheng, E. Zhang, L. Zhang and X. Wang, *Electrochim. Acta*, 2018, **263**, 391–399.
- 34 Q. Zhang, Z. Duan, M. Li and J. Guan, *Chem. Commun.*, 2020, **56**, 794–797.
- 35 L. Wu, Q. Li, C. H. Wu, H. Zhu, A. Mendoza-Garcia, B. Shen, J. Guo and S. Sun, *J. Am. Chem. Soc.*, 2015, **137**, 7071–7074.
- 36 B. M. Thamer, M. H. El-Newehy, S. S. Al-Deyab, M. A. Abdelkareem, H. Y. Kim and N. A. M. Barakat, *Appl. Catal., A*, 2015, **498**, 230–240.
- 37 C. C. Hou, W. F. Fu and Y. Chen, *ChemSusChem*, 2016, **9**, 2069–2073.
- 38 Z. Zhou, X. Li, Q. Li, Y. Zhao and H. Pang, *Mater. Today Chem.*, 2019, **11**, 169–196.
- 39 S. Francis, F. Leibsle, S. Haq, N. Xiang and M. Bowker, *Surf. Sci.*, 1994, **315**, 284–292.
- 40 P. Ferrin, A. U. Nilekar, J. Greeley, M. Mavrikakis and J. Rossmeisl, *Surf. Sci.*, 2008, **602**, 3424–3431.
- 41 T. Iwasita, H. Hoster, A. John-Anacker, W. F. Lin and W. Vielstich, *Langmuir*, 2000, **16**, 522–529.
- 42 S. L. Gojković, T. Vidaković and D. Đurović, *Electrochim. Acta*, 2003, **48**, 3607–3614.
- 43 Z. K. Ghouri, N. A. M. Barakat and H. Y. Kim, *Sci. Rep.*, 2015, **5**, 16695.
- 44 D. C. Sesu, P. Marbaniang, S. Ingavale, A. C. Manohar and B. Kakade, *ChemistrySelect*, 2020, **5**, 306–311.
- 45 C. Mattevi, H. Kim and M. Chhowalla, *J. Mater. Chem.*, 2011, **21**, 3324–3334.
- 46 M. Galaburda, E. Kovalska, B. T. Hogan, A. Baldycheva, A. Nikolenko, G. I. Dovbeshko, O. I. Oranska and V. M. Bogatyrov, *Sci. Rep.*, 2019, **9**, 17435.
- 47 S. Schwebke, U. Werner and G. Schultes, *J. Sens. Sens. Syst.*, 2018, **7**, 69–78.
- 48 J. Yoshihara and C. T. Campbell, *J. Catal.*, 1996, **161**, 776–782.